Mathematical modelling of pipe-flow and extrusion of composite materials

Problem presented by

Caroline Bird

Unilever Research

Study Group contributors

David Allwright (Smith Institute)
Chris Breward (University of Oxford)
John Byatt-Smith (University of Edinburgh)
Paul Dellar (University of Oxford)
Carina Edwards (University of Oxford)
Darren Fidler (Heriot-Watt University)
Marianne Grammatika (University of Sheffield)
Andrew Grief (University of Oxford)
John Hinch (University of Cambridge)
Katerina Kaouri (University of Oxford)
Arjen Koop (University of Oxford)
Gregory Kozyreff (University of Oxford)
Andrew Lacey (Heriot-Watt University)
John Ockendon (University of Oxford)
Colin Please (University of Southampton)
Giles Richardson (University of Nottingham)
Caroline Voong (Heriot-Watt University)
Stephen Wilson (University of Strathclyde)

Report prepared by

Chris Breward (University of Oxford)
Paul Dellar (University of Oxford)
Carina Edwards (University of Oxford)
Katerina Kaouri (University of Oxford)
Giles Richardson (University of Nottingham)
Stephen Wilson (University of Strathclyde)

1 Introduction

There exist a large number of industrial applications which involve the extrusion of aerated composite materials through an orifice, *e.g.* styrofoam, insulation, confectionery. Often such delicate structures change due to shear and pressure fields experienced on extrusion. In this work we investigate the influence of these shear and pressure fields on the structure of aerated composite materials, particularly the degree of aeration retained.

1.1 Material description

We consider our aerated composite to be a material comprising dispersed particles and air in a continuous fluid phase (particle free).

1.2 Model extruder

The extrusion is modelled as flow through a pipe of circular cross section followed by flow through an orifice of say 10 mm diameter. It is typically observed that, for a material of the kind described in the previous paragraph, the degree of aeration following passage through the orifice is significantly reduced.

2 Comparison of the flows for pipe and orifice

Neglecting separation of the various phases, the material behaves like a power law fluid with constitutive relation

$$\tau = \mu \dot{\gamma}^{1+\lambda}\,, \tag{2.1}$$

where τ is the deviatoric stress and $\dot{\gamma}$ is the strain rate (see section 5). The shear-thinning exponent used here is $\lambda = -0.42$. The "dynamic viscosity" μ has dimensions $[\mathrm{M}][\mathrm{L}]^{-1}[\mathrm{T}]^{\lambda-1}$ and the value chosen here is $200\,\mathrm{kg\,m^{-1}\,s^{-1.42}}$ in SI units.

We assumed the flow could be crudely modelled as a cylindrical Poiseuille-type flow merging into a spherical sink flow near the lower aperture. In Poiseuille-type flow of a power law fluid the pressure drop per unit length is given by (see section 5)

$$\frac{dp}{dz} \sim \mu \frac{Q^{1+\lambda}}{R^{4+3\lambda}}, \tag{2.2}$$

where Q is the volume flux, and R the cylinder's outer radius. For the values used here this evaluates to $1.3\,\mathrm{bar\,m^{-1}}$.

Near the aperture we assumed a spherical sink flow, in which

$$u \sim \frac{Q}{a^2}, \quad \text{so } \dot{\gamma} \sim \frac{Q}{a^3}, \quad \text{and } \tau \sim \rho\nu \left(\frac{Q}{a^3}\right)^{1+\lambda}, \tag{2.3}$$

where a is the radius of the aperture. Comparing these two estimates, we obtain a ratio

$$\frac{\Delta p_{\mathrm{pipe}}}{\Delta p_{\mathrm{sink}}} \sim \frac{L}{R}\left(\frac{a^3}{R^3}\right)^{1+\lambda \approx 0.58} \sim 0.15 \ll 1, \tag{2.4}$$

where Δp_{pipe} is the pressure drop along the length L of the cylinder, and Δp_{sink} the pressure drop in the vicinity of the aperture. We concluded that flow resistance occurs close to the aperture in the base of the cylinder. Also, the total pressure drop, $1.3\,\text{bar}\,\text{m}^{-1}$ for 0.07 m along the cylinder, plus $1/0.15 \approx 6.7$ times that across the aperture, is close to one bar. These crude estimates are refined in section 5, which studies self-similar solutions for spherically symmetric slow viscous inflow of a power law fluid in a cone. Note that the dimensionless group given by (2.4) is very sensitive to changes in the shear thinning exponent λ.

These estimates, and the more refined calculations in section 5, are based on the inertialess slow flow equation $\nabla \cdot \boldsymbol{\sigma} = 0$. In fact, from the volume flux Q and the "kinematic viscosity" $\nu = \mu/\rho$ we may form a lengthscale

$$\mathcal{L} = \left(\nu Q^{\lambda-1}\right)^{1/(3\lambda-1)}. \tag{2.5}$$

In spherically symmetric inflow $\mathcal{L}$ marks the radius below which the fluid velocity becomes large enough that inertial effects are significant. However, there is no such lengthscale $\mathcal{L}$ for the special case of a shear-thickening fluid with $\lambda = 1/3$. Thus a self-similar solution may be sought for the fully inertial equations $\rho D\mathbf{u}/Dt = \nabla \cdot \boldsymbol{\sigma}$. This represents the true axisymmetric analogue of Jeffery–Hamel flow of a Newtonian fluid in planar geometry, where a self-similar form exists for the full Navier-Stokes equations. Analysis of these self-similar solutions suggests that the slow flow approximation remains quantitatively accurate even when the nominal ratio of inertial to viscous terms is somewhat larger than unity.

3 Material composite modelling

We took several approaches to the modelling of the material, which we will describe in detail in the following sections. First we consider the material to be made up of two phases, particles and "particle-free", for simplicity. Then we will discuss the analogous model where we have air and "not air". Finally, we will consider a non-Newtonian model for the flow of the composite as a single phase.

3.1 Two-phase model for particles and particle-free

We write ϕ as the volume fraction of particles, and then our conservation of mass equations (treating each phase as incompressible) read

$$\frac{\partial \phi}{\partial t} + \nabla.\left(\mathbf{u}_1 \phi\right) = 0, \tag{3.6}$$

$$\frac{\partial (1-\phi)}{\partial t} + \nabla.\left(\mathbf{u}_2 (1-\phi)\right) = 0, \tag{3.7}$$

where $\mathbf{u}_1$ and $\mathbf{u}_2$ are the velocities of the particles and particle-free phases respectively. We then write down a balance of forces for each of the phases, noting that the Reynolds number for any macroscopic flow is small:

$$-\phi \nabla P_1 = D(\phi)\left(\mathbf{u}_1 - \mathbf{u}_2\right), \tag{3.8}$$

$$-(1-\phi)\nabla P_2 = -D(\phi)\left(\mathbf{u}_1 - \mathbf{u}_2\right), \tag{3.9}$$

where P_1 and P_2 are the pressures in the two phases (assuming that each phase is connected). Note that we have assumed for simplicity that the stress in each phase is "inviscid" and that the only effect of the viscosity is in the drag term. We may find appropriate forms for the drag coefficient, $D(\phi)$, by looking in, for example, [4]. In order to close our model we must impose a constitutive law which relates the pressures in the two phases. We pose the general form

$$P_1 - P_2 = f(\phi), \tag{3.10}$$

where f represents the excess pressure, which we might set to be

$$f = Ke^{-\phi/(1-\phi)}, \tag{3.11}$$

in line with expressions used in soil mechanics.

In order to see whether this model might predict particle blockage, we looked at the one-dimensional version of the governing equations:

$$\frac{\partial \phi}{\partial t} + \frac{\partial}{\partial x}\left(u_1\phi\right)_x = 0, \tag{3.12}$$

$$-\frac{\partial \phi}{\partial t} + \frac{\partial}{\partial x}\left(u_2(1-\phi)\right)_x = 0, \tag{3.13}$$

$$-\frac{\partial P_1}{\partial x} + (1-\phi)\frac{\partial f}{\partial \phi}\frac{\partial \phi}{\partial x} = 0, \tag{3.14}$$

$$-\phi\frac{\partial P_1}{\partial x} = D(\phi)(u_1 - u_2). \tag{3.15}$$

Note that we have added (3.8) and (3.9) together to yield (3.14). In this configuration, we consider sliding along a tube. We impose the velocity with which we move the piston, and we specify the pressure at the open end of the tube,

$$u_1 = u_2 = U \qquad \text{at} \qquad x = Ut, \tag{3.16}$$

$$P_1 = P_{\text{atm}} \qquad \text{at} \qquad x = L, \tag{3.17}$$

and we assume initially that the material has a constant composition, so that

$$\phi = \phi_0 \qquad \text{at} \qquad t = 0. \tag{3.18}$$

We add (3.12) and (3.13), integrate, and apply the boundary conditions to find that

$$\phi u_1 + (1-\phi)u_2 = U. \tag{3.19}$$

We seek a travelling wave solution and thus, noting that the wave speed must be U in order to satisfy the boundary conditions, we set $\xi = x - Ut$, to find that

$$\left((u_1 - U)\phi\right)_\xi = 0, \tag{3.20}$$

$$-\frac{\partial P_1}{\partial \xi} + (1-\phi)\frac{\partial f}{\partial \phi}\frac{\partial \phi}{\partial \xi} = 0, \tag{3.21}$$

$$\phi\frac{\partial P_1}{\partial \xi} = D(\phi)(u_1 - u_2). \tag{3.22}$$

Integrating (3.20), we find that

$$(u_1 - U)\phi = \text{constant} = 0, \tag{3.23}$$

when we apply the boundary conditions. We conclude that $u_1 = U$. Substituting this into (3.19), we find that $u_2 = U$. Equation (3.22) reveals that the pressure is constant; (3.21) then has the solution ϕ is constant.

We conclude that the composite material merely translates to the right with no change of composition. Clearly our one-dimensional two-phase model is too gross a simplification to capture any particle separation.

4 Squeezing out the air bubbles

4.1 A mathematical model

In an attempt to model the preferential squeezing out of the air bubbles we formulated a two-phase model for the composite material consisting of air bubbles (phase 1) and "not-air", *i.e.* everything else (phase 2). Evidently this model will have some similarities to (but be essentially different from) the two-phase particle and "particle-free" model described in section 2. Phase 1 is assumed to be "inviscid" (as in section 2) but phase 2 is assumed to be "viscous" with viscosity μ_2. Let us assume that the material is being driven out of the extruder by a piston. Unlike in section 2 we assume that, since the typical squeezing pressures are greatly in excess of typical pressures due to surface tension, the pressures in the two phases are equal, *i.e.* $p_1 = p_2 = p$. Furthermore, we assume that the pressures are so large that phase 1 (but not the much denser phase 2) is compressible with non-uniform density ρ and adopt the simple isothermal gas law $p = k\rho$ (since the mass of the dense phase is so much greater than of the air, it will act like a heat buffer). Using subscripts 1 and 2 to denote quantities in the two phases and ϕ to denote the volume fraction of air then (assuming that inertial effects are negligible in both phases) the statements of conservation of mass of air, mass of not-air, momentum of air and momentum of not-air take the forms

$$(\rho\phi)_t + \nabla\cdot(\rho\phi\mathbf{u}_1) = 0, \tag{4.24}$$

$$(1-\phi)_t + \nabla\cdot[(1-\phi)\mathbf{u}_2] = 0, \tag{4.25}$$

$$-k\phi\nabla\rho = D(\phi)(\mathbf{u}_1 - \mathbf{u}_2), \tag{4.26}$$

$$-k(1-\phi)\nabla\rho + \mu_2\nabla\cdot[(1-\phi)\nabla\mathbf{u}_2] = -D(\phi)(\mathbf{u}_1 - \mathbf{u}_2). \tag{4.27}$$

4.2 Solution procedure

In order to make analytical progress we consider flow in a *slowly varying channel*, in which case the appropriately scaled and non-dimensionalised leading order version of

equations (4.24)–(4.27) are

$$(\rho\phi)_t + (\rho\phi u_1)_x + (\rho\phi v_1)_y = 0, \tag{4.28}$$
$$(1-\phi)_t + \left[(1-\phi)u_2\right]_x + \left[(1-\phi)v_2\right]_y = 0, \tag{4.29}$$
$$-k\phi\rho_x = d(\phi)(u_1 - u_2), \tag{4.30}$$
$$-k(1-\phi)\rho_x + \left[(1-\phi)u_{2y}\right]_y = -d(\phi)(u_1 - u_2), \tag{4.31}$$

where $\rho = \rho(x,t)$, $\phi = \phi(x,t)$ and d is the nondimensional form of D.

Adding (4.30) and (4.31) yields

$$-k\rho_x + \left[(1-\phi)u_{2y}\right]_y = 0, \tag{4.32}$$

which can be integrated twice with respect to y to yield

$$u_2 = \frac{k\rho_x(y^2 - hy)}{2(1-\phi)} \tag{4.33}$$

satisfying the no-slip boundary conditions $u_2(0) = u_2(h) = 0$, and so from (4.30)

$$u_1 = k\rho_x \left[\frac{y^2 - hy}{2(1-\phi)} - \frac{\phi}{d(\phi)}\right]. \tag{4.34}$$

If the channel is bounded by solid walls at $y = 0$ and $y = h(x)$ then averaging equations (4.28) and (4.29) across the channel yields

$$(h\rho\phi)_t + (h\rho\phi\bar{u}_1)_x = 0, \tag{4.35}$$
$$\left[h(1-\phi)\right]_t + \left[h(1-\phi)\bar{u}_2\right]_x = 0, \tag{4.36}$$

where $\bar{u}_1$ and $\bar{u}_2$ are average values of u_1 and u_2 defined by

$$\bar{u}_1 = \frac{1}{h}\int_0^h u_1 \, \mathrm{d}y = -k\rho_x \left[\frac{h^2}{12(1-\phi)} + \frac{\phi}{d(\phi)}\right], \quad \bar{u}_2 = \frac{1}{h}\int_0^h u_2 \, \mathrm{d}y = -\frac{k\rho_x h^2}{12(1-\phi)}. \tag{4.37}$$

Thus in steady flow (4.36) implies that the pressure gradient $p_x = k\rho_x$ satisfies the Reynolds equation

$$p_x = -\frac{12Q_2}{h^3}, \tag{4.38}$$

where the value of the constant Q_2 is determined by imposing the boundary conditions $p(0) = 1 + \Delta P$ and $p(1) = 1$ on (4.38), that is

$$p = 1 + \Delta P - 12Q_2 \int_0^x \frac{1}{h^3} \, \mathrm{d}x, \quad Q_2 = +\frac{\Delta P}{12\displaystyle\int_0^1 \frac{1}{h^3} \, \mathrm{d}x}. \tag{4.39}$$

On the other hand (4.35) implies that ϕ satisfies the algebraic equation

$$-\frac{h\phi p p_x}{k}\left[\frac{h^2}{12(1-\phi)} + \frac{\phi}{d(\phi)}\right] = Q_1, \tag{4.40}$$

where Q_1 is a constant. Hereafter we will take $d(\phi) \equiv 1$ for simplicity, but more complicated functions could be treated in the same way. At atmospheric pressure, we assume here that the volume fraction of the air content is 1/2. When we increase the pressure at the piston to $1 + \Delta P$, the air contracts while the volume of the "not-air" remains constant. The resulting volume fraction which will serve as our boundary condition at the piston is then given by $\phi(0) = 1/(2 + \Delta P)$. We use this condition along with $h(0) = 1$ and $p(0) = 1 + \Delta P$ to yield

$$Q_1 = \frac{Q_2}{k}\left(1 + \frac{12(1+\Delta P)}{(2+\Delta P)^2}\right) \tag{4.41}$$

and hence (4.40) becomes

$$\phi p\left[\frac{1}{12(1-\phi)} + \frac{\phi}{h^2}\right] = \frac{1}{12} + \frac{1+\Delta P}{(2+\Delta P)^2} = g(\Delta P). \tag{4.42}$$

In particular, equation (4.42) yields a cubic equation for $\phi(1) = \phi_1$ in terms of ΔP and $h(1) = h_1$:

$$\phi_1^3 - \phi_1^2 - \phi_1 h_1^2\left(g + \frac{1}{12}\right) + h_1^2 g = 0. \tag{4.43}$$

4.3 Solution for a uniform channel

In the simplest case of a uniform channel, $h = 1$, then from (4.39) we have

$$p = 1 + \Delta P - 12Q_2 x, \quad Q_2 = +\frac{\Delta P}{12}, \tag{4.44}$$

and so

$$p = 1 + \Delta P(1 - x), \tag{4.45}$$

and hence from (4.42) ϕ satisfies

$$\phi(1 + \Delta P(1-x))\left[\frac{1}{12(1-\phi)} + \phi\right] = g(\Delta P). \tag{4.46}$$

Figure 1 shows ϕ plotted as a function of x for a range of values of ΔP, and figure 2 shows $\phi(1)$ plotted as a function of ΔP. Figures 1 and 2 show us that ϕ monotonically increases as x increases, indicating that the air close to the piston contracts. We also see that ϕ decreases everywhere as ΔP increases. We see that $\phi(1) < 1/2$ always, representing the fact that the air is preferentially squeezed out.

4.4 Solution for a sloped channel

In the case of a channel with a sloped wall, $h = 1 - \alpha x$ ($\alpha \leq 1$), then from (4.39) we have

$$p = 1 - \frac{6Q_2\left[1 - (1-\alpha x)^2\right]}{\alpha(1-\alpha x)^2}, \quad Q_2 = \frac{\Delta P \alpha(1-\alpha)^2}{6\left[1 - (1-\alpha)^2\right]}, \tag{4.47}$$

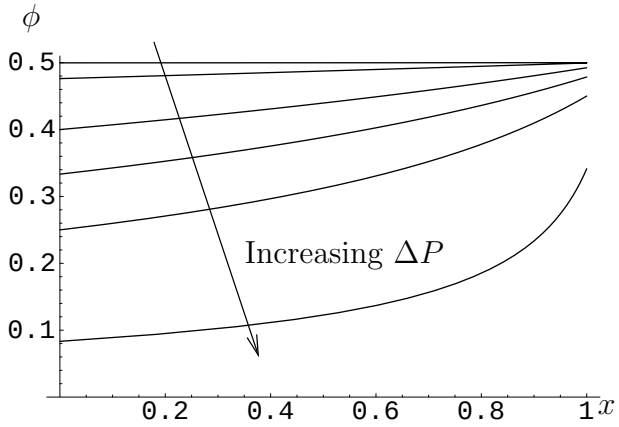

Figure 1: Numerically calculated values of ϕ plotted as a function of x for $\Delta P = 0$ (highest curve), 0.1, 0.5, 1, 2 and 10 (lowest curve) for a uniform channel, $h = 1$.

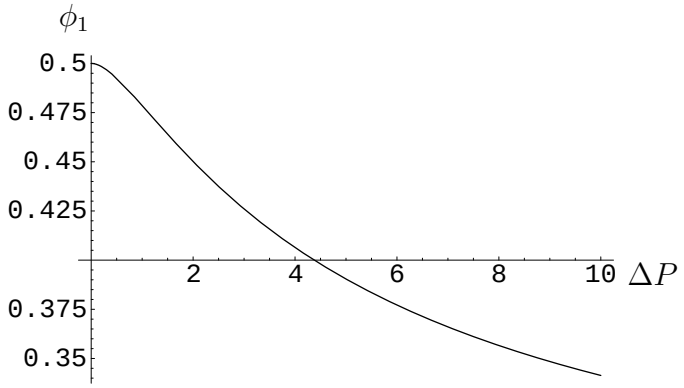

Figure 2: Numerically calculated values of ϕ_1 plotted as a function of ΔP for a uniform channel, $h = 1$.

and so

$$p = 1 + \Delta P - \Delta P \left(\frac{1-\alpha}{1-\alpha x} \right)^2 \frac{1-(1-\alpha x)^2}{1-(1-\alpha)^2}, \tag{4.48}$$

and hence from (4.42) ϕ satisfies

$$\phi \left[1 + \Delta P - \Delta P \left(\frac{1-\alpha}{1-\alpha x} \right)^2 \frac{1-(1-\alpha x)^2}{1-(1-\alpha)^2} \right] \left[\frac{1}{12(1-\phi)} + \frac{\phi}{(1-\alpha x)^2} \right] = g(\Delta P). \tag{4.49}$$

Figure 3 shows ϕ plotted as a function of x for a range of values of α when (a) $\Delta P = 0.1$, (b) $\Delta P = 1$, and (c) $\Delta P = 10$, and figure 3(d) shows $\phi(1) = \phi_1$ plotted as a function of ΔP for a range of values of α. Figures 3 and 4 show that varying α can have a dramatic effect on the preferential squeezing out of the air. In particular, figure 3(d) shows that *increasing* α always has the effect of *decreasing* $\phi(1)$.

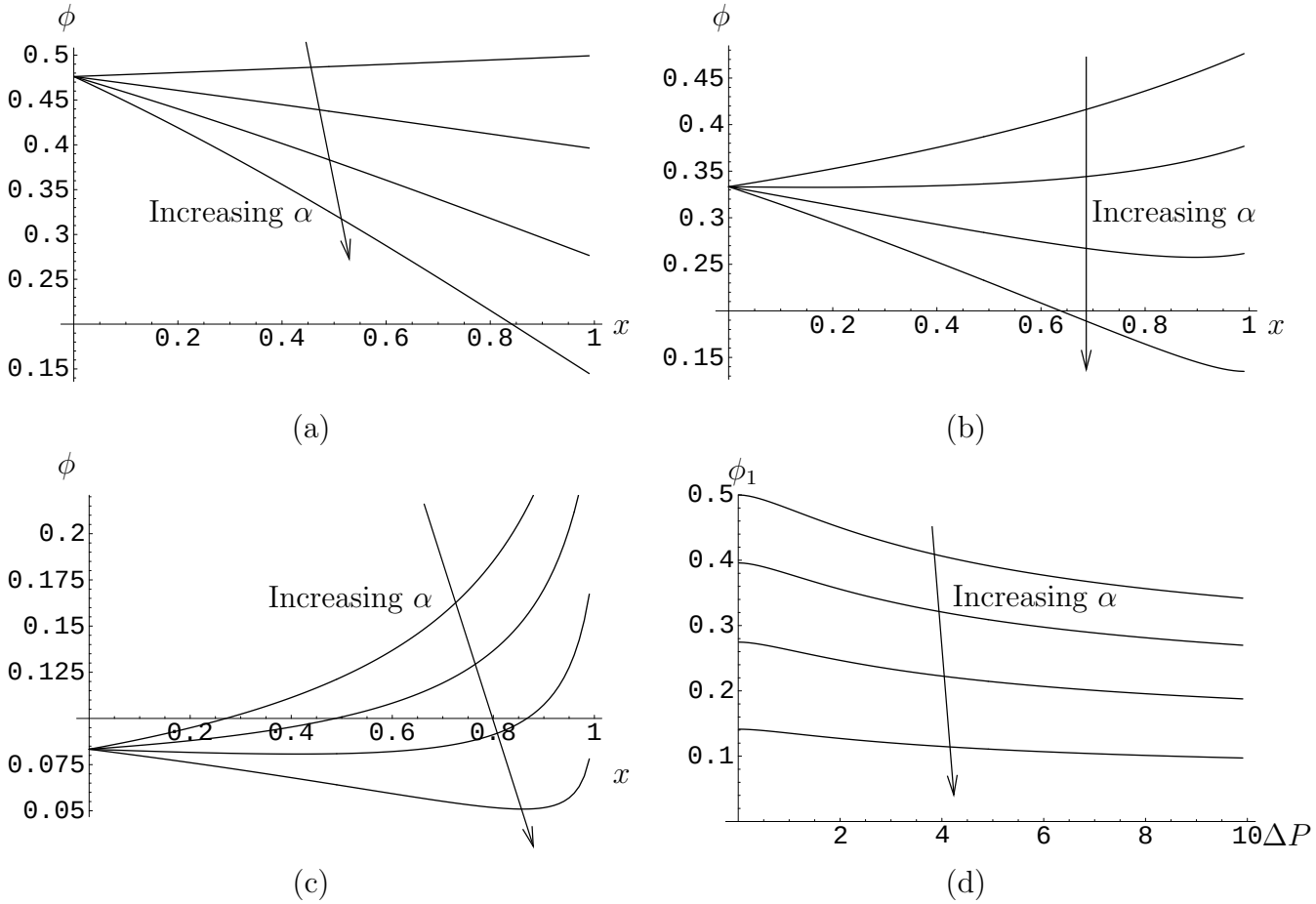

Figure 3: (a) Graph showing how ϕ varies with x, when $\Delta P = 0.1$. (b) Graph showing how ϕ varies with x, when $\Delta P = 1$. (c) Graph showing how ϕ varies with x, when $\Delta P = 10$. (d) Graph showing how $\phi(1) = \phi_1$ varies with ΔP. In each case, we have used $\alpha = 0$, 0.25, 0.5, and 0.75.

4.5 Conclusions

In this section we have developed a two-phase model for the air and "not-air" which make up a composite material capable of capturing the preferential squeezing out of the air often observed in practice. Analysing the model suggests that altering the shape of the channel can have a dramatic effect on the squeezing out of the air. We note that it should be possible to engineer the channel so as to achieve a desired volume fraction of air at the exit. It would be very interesting to test the predictions of the present model against experimental observations.

5 Jeffery-Hamel-style flow of a power-law fluid in a cone

Realistic calculations of the flow of a composite material through an extruder can only be made using numerical methods beyond the scope of this report. We can, however, get

some insight into the flow by considering the following scenario in which the composite material is placed in a cone, of semi-vertical angle β, and forced out through a small orifice close to the apex of the cone (see figure 4). Our aim is to calculate the power required to sustain such flow (and compare with a similar flow in a cylinder) since this gives a guide to the feasibility of extruding a composite material from its container. We expect the flow to be approximately spherically symmetric away from the orifice and the forced surface. Since the flow is divergence free and satisfies no slip boundary conditions on the edge of the cone, this implies that the flow velocity takes the form

$$\boldsymbol{u} = \frac{f(\theta)}{r^2}\boldsymbol{e}_r, \tag{5.50}$$

where (r, θ, ϕ) are the standard spherical polar coordinates. This is a Jeffery-Hamel flow (Jeffery-Hamel flow in a wedge for a power law fluid is considered in [2]). We model the material as a single phase shear thinning power-law fluid. The stress tensor σ hence takes the form

$$\sigma_{ij} = -p\delta_{ij} + \tau_{ij},$$

where the deviatoric part of the stress tensor has the form

$$\tau_{ij} = 2\mu_0(\dot{\gamma})^{\lambda} e_{ij}. \tag{5.51}$$

Here e_{ij} is the the strain tensor,

$$\dot{\gamma} = |2e_{ij}e_{ij}|^{1/2}$$

and λ is the power law exponent. Note that $\lambda = 0$ corresponds to a Newtonian fluid, $\lambda < 0$ to a shear thinning fluid and $\lambda > 0$ to a shear thickening fluid. Furthermore we shall assume that inertia is negligible so that the slow flow equation

$$\sigma_{ij,j} = 0 \tag{5.52}$$

holds.

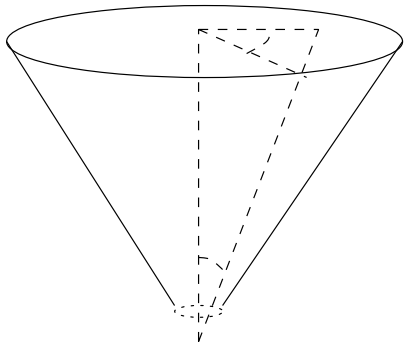

Figure 4: The setup and coordinate system being considered.

For the flow (5.50) the strain rate is

$$\dot{\gamma} = \frac{\alpha(\theta)}{r^3}, \quad \text{where} \quad \alpha = (12f^2 + f'^2)^{1/2}$$

and the components of the stress tensor are

$$\begin{aligned} \sigma_{rr} &= -4\mu_0 \frac{\alpha^\lambda f}{r^{3+3\lambda}} - p, \quad \sigma_{\theta\theta} = 2\mu_0 \frac{\alpha^\lambda f}{r^{3+3\lambda}} - p, \quad \sigma_{\phi\phi} = \sigma_{\theta\theta}, \\ \sigma_{r\theta} &= \mu_0 \frac{\alpha^\lambda f'}{r^{3+3\lambda}}, \qquad\qquad \sigma_{r\phi} = 0, \qquad\qquad \sigma_{\theta\phi} = 0. \end{aligned} \tag{5.53}$$

In spherical polar coordinates the slow flow equation (5.52) may be rewritten as

$$\begin{aligned} &\frac{1}{r^2}\frac{\partial}{\partial r}\left(r^2\sigma_{rr}\right) + \frac{1}{r\sin\theta}\frac{\partial}{\partial\theta}\left(\sin\theta\sigma_{r\theta}\right) - \frac{\sigma_{\theta\theta}+\sigma_{\phi\phi}}{r} + \frac{1}{r\sin\theta}\frac{\partial\sigma_{r\phi}}{\partial\phi} = 0, \\ &\frac{1}{r^2}\frac{\partial}{\partial r}\left(r^2\sigma_{r\theta}\right) + \frac{1}{r\sin\theta}\frac{\partial}{\partial\theta}\left(\sin\theta\sigma_{\theta\theta}\right) + \frac{\sigma_{r\theta}}{r} + \frac{1}{r\sin\theta}\frac{\partial\sigma_{\theta\phi}}{\partial\phi} - \frac{\cot\theta}{r}\sigma_{\phi\phi} = 0, \\ &\frac{1}{r^2}\frac{\partial}{\partial r}\left(r^2\sigma_{r\phi}\right) + \frac{1}{r\sin\theta}\frac{\partial}{\partial\theta}\left(\sin\theta\sigma_{\theta\phi}\right) + \frac{1}{r\sin\theta}\frac{\partial\sigma_{\phi\phi}}{\partial\phi} + \frac{\cot\theta}{r}\sigma_{\theta\phi} + \frac{\sigma_{r\phi}}{r} = 0. \end{aligned} \tag{5.54}$$

Since there is no ϕ-dependence in the problem, the third momentum equation is redundant and we ignore it henceforth. On substituting (5.53) into (5.54) we obtain the following coupled equations for f and p:

$$\frac{\partial p}{\partial r} = 2\mu_0 r^{-(4+3\lambda)}\left(6\lambda\alpha^\lambda f + \frac{1}{2\sin\theta}\frac{d}{d\theta}\left(\sin\theta\alpha^\lambda\frac{df}{d\theta}\right)\right), \tag{5.55}$$

$$\frac{\partial p}{\partial\theta} = 2\mu_0 r^{-(3+3\lambda)}\left(-\frac{3\lambda}{2}\alpha^\lambda\frac{df}{d\theta} + \frac{d}{d\theta}(\alpha^\lambda f)\right). \tag{5.56}$$

The pressure can be eliminated in the standard way by cross differentiation (*i.e.* forming the vorticity equation) and this leads to a third-order ODE for f:

$$\begin{aligned} &\frac{d}{d\theta}\left(\frac{1}{\sin\theta}\frac{d}{d\theta}\left(\sin\theta\alpha^\lambda\frac{df}{d\theta}\right)\right) + (6+18\lambda)\frac{d}{d\theta}\left(\alpha^\lambda f\right) - 3\lambda(3+3\lambda)\alpha^\lambda\frac{df}{d\theta} = 0, \\ &\alpha = (12f^2 + f'^2)^{1/2}, \end{aligned} \tag{5.57}$$

which must be solved together with the boundary conditions

$$f(\beta) = 0, \quad \frac{df}{d\theta}(0) = 0, \quad 2\pi\int_0^\beta \sin\theta f(\theta)d\theta = -Q. \tag{5.58}$$

Here the first condition is the no-slip condition enforced on the edge of the cone, the second a symmetry condition and the third specifies the flux Q down through the cone. Since (5.57) is homogeneous in f, we choose instead to solve (5.57) for $\widehat{f}$ with the boundary conditions

$$\widehat{f}(\beta) = 0, \quad \widehat{f}'(0) = 0 \quad \widehat{f}(0) = -1. \tag{5.59}$$

Note that f is related to $\widehat{f}$ by

$$f = -\frac{Q}{2\pi\int_0^\beta \sin\theta\widehat{f}d\theta}\widehat{f}$$

and hence that $\widehat{f}$ is dimensionless. Before proceeding with the numerical solution, we consider two special cases that arise for specific λ. First, we consider $\lambda = 0$, which corresponds to the case where we have a Newtonian fluid. Equation (5.57) becomes

$$\left(\frac{1}{\sin\theta}(f'\sin\theta)'\right)' + 6f' = 0, \tag{5.60}$$

which we can immediately integrate once to yield

$$\frac{1}{\sin\theta}(f'\sin\theta)' + 6f = C, \tag{5.61}$$

where C is an arbitrary constant. Applying the transformation $x = \cos\theta$, where $-1 \leq x \leq 1$, we have

$$(1-x^2)\frac{d^2f}{dx^2} - 2x\frac{df}{dx} + 6f = C. \tag{5.62}$$

Note that (5.62) is an inhomogeneous Legendre equation. Its solution f is given by

$$f(x) = A_0P_2(x) + B_0Q_2(x) + \frac{C}{6}, \tag{5.63}$$

where $P_2(x) = (3x^2-1)/2$ and $Q_2(x) = (3x^2-1)(\ln(1+x) - \ln(1-x))/4 - 3x/2$, and the constants A_0, B_0 and C_0 are uniquely determined by the boundary conditions (and B_0 must be zero for the solution to be regular at the origin). Note that we generate this solution so that we can check that our solution for general λ reduces to this solution when we set $\lambda = 0$.

There is another special case that we may consider, namely $\lambda = -1/3$. In this case, defining $g = \alpha^{-1/3}f'$, we have

$$\left(\frac{1}{\sin\theta}(g\sin\theta)'\right)' + 2g = 0. \tag{5.64}$$

In this case, our transformed problem reads

$$(1-x^2)\frac{d^2g}{dx^2} - 2x\frac{dg}{dx} + \left(2 - \frac{1}{1-x^2}\right)f = 0, \tag{5.65}$$

which has solution

$$g(x) = A_1{P_1}^1(x) + B_1{Q_1}^1(x), \tag{5.66}$$

where

$${P_1}^1(x) = (1-x^2)^{1/2}\frac{d}{dx}P_1(x) = (1-x^2)^{1/2}, \tag{5.67}$$

$${Q_1}^1(x) = (1-x^2)^{1/2}\frac{d}{dx}Q_1(x) = \frac{(1-x^2)^{1/2}}{2}\ln\left(\frac{1+x}{1-x}\right) - x(1-x^2)^{-1/2}, \tag{5.68}$$

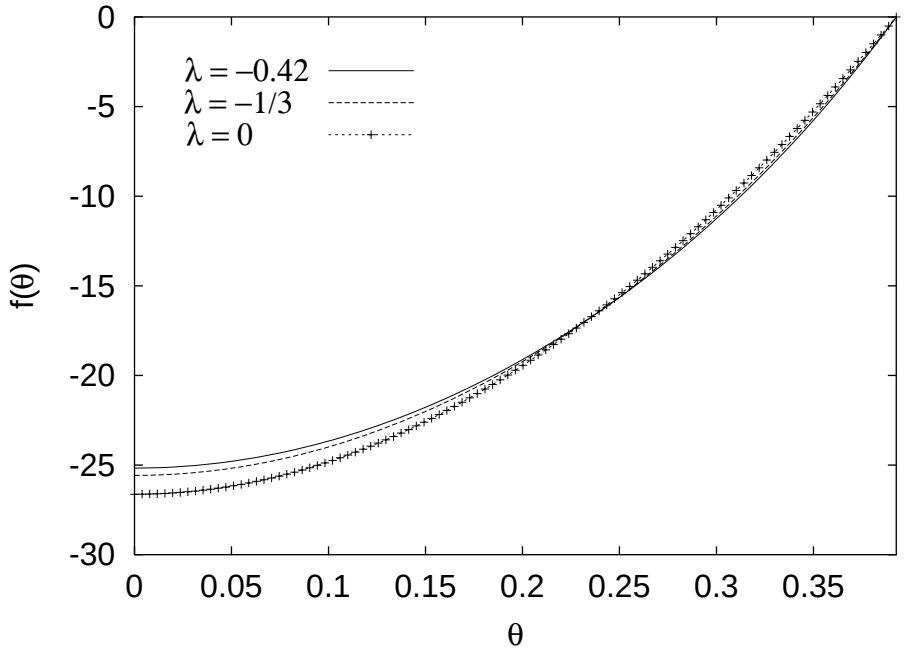

Figure 5: Figure showing $f(\theta)$ for fixed volume flux $Q = 1$ for three values of exponent λ.

and B_1 is found to be zero because we require the solution to be bounded as we approach the axis of symmetry. This specifies the first integral; the resulting equation must be solved numerically with the remaining boundary conditions to yield the functional form for the velocity.

Numerical solution of (5.57) requires that we account for the singular point of the equation at $\theta = 0$. The correct behaviour of $\widehat{f}$ close to the origin, which ensures $\widehat{f}'(0) = 0$, is

$$\widehat{f} \sim -1 + M\theta^2, \qquad \text{as } \theta \to 0,$$

where M is a constant determined by the condition $\widehat{f}(\beta) = 0$.

We note that the pressure in this flow is given by

$$p = -2\mu_0 \frac{r^{-(3+3\lambda)}}{3+3\lambda} \left(6\lambda\alpha^\lambda f + \frac{1}{2\sin\theta} \frac{d}{d\theta} \left(\sin\theta \alpha^\lambda \frac{df}{d\theta} \right) \right) + p_0, \tag{5.69}$$

where p_0 is a constant. We show the solution to (5.57) for the three values of the shear thinning exponent λ that we have considered so far in this report, namely $\lambda = 0$, $-1/3$ and -0.42, in figure 5. We see that changing the exponent has very little effect on the solution.

5.1 The power required to sustain the flow

When discussing pipe flows it is conventional to talk about the pressure drop between the ends of the pipe. This gives a measure of the resistance to flow in the pipe since a balance

of forces exerted in the direction of the flow equates the pressure drop multiplied by the cross sectional area of the pipe with the viscous forces exerted on the pipe walls, see section 5.2. Furthermore the power required to sustain the flow is just the pressure drop multiplied by the fluid flux. In contrast to pipe flow, there is no analogue of pressure drop for flow in a converging channel which would give a measure of resistance to flow (since the walls are non-parallel). As we wish to consider flow in a cone sustaining a radial spherically symmetric flow we thus consider power as a measure of the effort required, in particular we consider the power required to sustain the flow between radius a and radius b where $a > b$.

We would like to use the solution to (5.57) to get an estimate of the power required to force the flow through the cone. The power expended per unit area on a surface with normal $\boldsymbol{e}_r$ is $(\sigma \cdot \boldsymbol{e}_r) \cdot \boldsymbol{u}$, which we can express in the form $\sigma_{rr} f(\theta)/r^2$ (we note that we now need only work with one component of the stress tensor, σ_{rr}). It follows that the total power W expended to sustain the flow between the surfaces $r = a$ and $r = b$ $(0 \leq \theta \leq \beta)$ is

$$W = H(a) - H(b), \quad \text{where} \quad H(r) = 2\pi \int_0^\beta \sigma_{rr} f \sin\theta d\theta. \tag{5.70}$$

We can use (5.53) and (5.69) to re-express H in the form

$$H(r) = \frac{2\mu_0}{r^{3+3\lambda}} \left[2\pi \int_0^\beta \frac{f}{(6+6\lambda)} \left(\frac{d}{d\theta} \left(\sin\theta \alpha^\lambda f' \right) - 12\alpha^\lambda f \sin\theta \right) d\theta \right]. \tag{5.71}$$

Since we solve for $\widehat{f}$ it is convenient to leave this result in the following form

$$H(r) = \frac{2\mu_0 Q^{2+\lambda}}{r^{3+3\lambda}} \widetilde{H}(\beta, \lambda), \tag{5.72}$$

where the (negative) dimensionless parameter $\widetilde{H}$ is given by

$$\widetilde{H}(\beta, \lambda) = \pi \left[-\frac{1}{2\pi \int_0^\beta \sin\theta \widehat{f} d\theta} \right]^{2+\lambda} \int_0^\beta \frac{\widehat{f}}{3+3\lambda} \left(\frac{d}{d\theta} \left(\sin\theta \widehat{\alpha}^\lambda \widehat{f}' \right) - 12\widehat{\alpha}^\lambda \widehat{f} \sin\theta \right) d\theta. \tag{5.73}$$

So for example when we calculate the solution for $\widehat{f}$ in the case where the cone angle $\beta = \pi/8$ and the power law exponent $\lambda = -0.42$ we find

$$\widetilde{H}(\beta, \lambda = -0.42) \approx -12.1. \tag{5.74}$$

5.2 Comparison with flow in a cylinder

Shear-thinning flow in a cylinder is well documented (see for example Bird, Armstrong and Hassager [1]). Here we use cylindrical polars (r, θ, z) and the flow has the form

$$\boldsymbol{u} = g(r)\boldsymbol{e}_z. \tag{5.75}$$

The only non-zero components of the stress are

$$\sigma_{rr} = \sigma_{\theta\theta} = \sigma_{zz} = -p, \quad \sigma_{rz} = 2\mu_0(-g')^\lambda. \tag{5.76}$$

If the flow satisfies the slow flow equations (5.52) and the no-slip boundary condition is applied on $r = \rho$ then

$$g = \frac{\lambda+1}{\lambda+2}\left(\frac{k}{2\mu_0}\right)^{1/(\lambda+1)}\left(\rho^{(\lambda+2)/(\lambda+1)} - r^{(\lambda+2)/(\lambda+1)}\right), \quad p = kz, \tag{5.77}$$

and the flux Q down the pipe is given by

$$Q = \pi\frac{\lambda+1}{3\lambda+4}\left(\frac{k}{2\mu_0}\right)^{1/(\lambda+1)}\rho^{(3\lambda+4)/(\lambda+1)}. \tag{5.78}$$

This also gives

$$\frac{dp}{dz} = k = \left(\frac{3\lambda+4}{\pi(\lambda+1)}\right)^{\lambda+1}\frac{Q^{\lambda+1}}{\rho^{3\lambda+4}}, \tag{5.79}$$

as used in Section 2.

The power required to sustain the flow between $z = 0$ and $z = L$ is

$$W = \left[-2\pi\int_0^\rho \sigma_{zz}g(r)rdr\right]_{z=0}^{z=L} = kLQ \tag{5.80}$$

and hence

$$W = 2\mu_0\frac{LQ^{\lambda+2}}{\rho^{3\lambda+4}}\left(\frac{1}{\pi}\left(\frac{3\lambda+4}{\lambda+1}\right)^{\lambda+1}\right). \tag{5.81}$$

We note that the power, W, for a cylinder is directly proportional to $L = b-a$, while for the cone $W \propto b^{-(3+3\lambda)} - a^{-(3+3\lambda)}$ and as such depends on the shear-thinning exponent.

5.3 Conclusions

We have looked at slow flow of a power law fluid with exponent λ down a cone. Assuming spherical symmetry, in the style of Jeffery-Hamel flow, the equations of motion reduce to a single, nonlinear, ordinary differential equation (5.57) for $f(\theta)$. For Newtonian flow, $\lambda = 0$, an exact solution (5.63) was obtained which served as a check on any results obtained for non-Newtonian flow. For the particular case of $\lambda = -1/3$ it is interesting that a first integral of equation (5.57) can be obtained analytically.

To proceed further it was necessary to solve equation (5.57) numerically, and a solution for $\widehat{f}$ was derived for the particular value of $\lambda = -0.42$ (see figure 5). Considering power as a measure of the effort required to drive the flow, the expression (5.71) was obtained, and evaluated for the semi-vertical angle $\beta = \pi/8$. We finally note that the numerical solution for $f(\theta)$ allows all components of the stress tensor and indeed all flow quantities to be calculated.

6 Conclusions

We formulated several models to describe the extrusion of aerated composite materials. First, we looked at whether it was easier to get the material down the pipe or out through

the orifice, and we concluded that the main resistance to flow was in getting the material out through the orifice. Then we described the motion of the material as a two-phase flow, in which the two phases were particles and particle-free. In a one-dimensional model, the material merely translated, with no change in composition. We then formulated a model for describing the motion of air bubbles. We formulated a two-phase model, but here we considered a slender block of material. The resulting "thin film" model was solved, and it was seen that the geometry of the channel was very important. We ended up with a solution in which the volume fraction of air was not constant throughout the block. We postulated that, by a crafty choice of channel shape, it ought to be possible to control the volume fraction of air at the exit of the tube. Finally, we formulated a model to describe the flow of a one-phase power-law fluid in a cone. We were able to calculate the power required to move the material down the cone.

There are several areas to follow up, including:

1. We could re-do the calculations for particles/particle-free in a two-dimensional geometry, to see whether or not the shape of the channel could affect the volume fractions, as it did in the air/not air case.

2. We could alter the power-law fluid flow to incorporate stress-free boundary conditions (modelling the flow of the material between two corner vortices and towards the orifice). Further, we could incorporate a yield stress into our formulation, to see what effect this would have.

References

[1] R.B. Bird, R.C. Armstrong and C. Hassager. *Dynamics of Polymeric fluids Volume 1.* Wiley (1987).

[2] S.J. Chapman, A.D. Fitt and C.P. Please. Extrusion of power law shear thinning fluids with small exponent. *International Journal of Nonlinear Mechanics*, **32**, 187-199 (1997).

[3] A.D. Fitt, P.D. Howell, J.R. King, C.P. Please and D.W. Schwendeman. Poroelastic multiphase flow modelling for paper squeezing. *Euro. J. Appl. Maths*, to appear (2002).

[4] A.C. Fowler. *Mathematical models in the applied sciences.* Cambridge University Press, Cambridge. (1997)